Structure and Electrochemistry of Heterobimetallic Ferrocenecarboxylatoruthenium(II) Complexes

Ian W. Wyman,[†] Tara J. Burchell,[†] Kathy N. Robertson,[‡] T. Stanley Cameron,[‡] and Manuel A. S. Aquino*,[†]

Department of Chemistry, St. Francis Xavier University, P.O. Box 5000, Antigonish, Nova Scotia, B2G 2W5, Canada, and Department of Chemistry, Dalhousie University, Halifax, Nova Scotia, B3H 4J3, Canada

Received May 21, 2004

The mixed-valent diruthenium complexes $[Ru_2(\mu\text{-}O_2CR)_4L_2](PF_6)$ (where R = CH_3, L = H_2O or R = Fc (ferrocenyl), L = MeOH) were reacted with the three diphosphine (dpp) ligands bis(diphenylphosphino)methane (dppm), 1,2-bis(diphenylphosphino)ethane (dppe), and 1,3-bis(diphenylphosphino)propane (dppp) to yield, via a disassembly reaction, the monoruthenium(II) complexes $[Ru(\eta^2\text{-}O_2CR)(dpp)_2](PF_6)$ (R = CH_3 and dpp = dppm (**1**), dpp = dppe (**2**), dpp = dppp (**3**); R = Fc and dpp = dppm (**4**), dpp = dppe (**5**), dpp = dppp (**6**)). All six complexes were characterized by elemental analysis, IR and NMR (^1H and ^{31}P) spectroscopy, cyclic and Osteryoung square wave voltammetry, and X-ray crystallography. Complexes **4**−**6** are rare examples of structurally characterized ruthenium complexes with η^2-bound ferrocenecarboxylate ligands, and they are unique in displaying a metal and an organometallic center. The electrochemical measurements reveal an essentially reversible ruthenium-centered redox process for complexes **2** and **3**, which becomes irreversible in the presence of the ferrocenyl group in complexes **4**−**6**. The iron-centered redox process in complexes **4**−**6** is chemically reversible. The separation between these redox processes is large (>1.0 V), leading to a stable "mixed-valent" state, and increases in the potential separation of these two redox processes over the separation seen between the redox potentials of the isolated ruthenium and ferrocenecarboxylate fragments may indicate the possibility of metal−metal interactions. A mechanism for the disassembly process, exploited in the synthetic procedure, is postulated.

Introduction

It has been well documented that the reaction of the mixed-valent diruthenium(II,III) tetracarboxylate core, $[Ru_2(\mu\text{-}O_2CR)_4]^+$ where R is normally an alkyl or aryl group, with π-acid phosphine ligands leads to a breakdown in the "paddle-wheel" structure with loss or rearrangement of some or all of the carboxylate groups as well as Ru−Ru bond cleavage.[1−10] The final products of this "disassembly" process often depends on the reaction conditions used.

Early reactions with monophosphine ligands, such as PPh_3, produced oxo-bridged di- and triruthenium(III) complexes in which the Ru−Ru bond was lost, the carboxylates were bound in both μ_2 and η^2 fashions, and the PPh_3 ligands were bound in equatorial positions.[2−4] Subsequently Jiménez-Aparicio and co-workers[5] reacted PPh_3 with $[Ru_2(\mu\text{-}O_2CCH_3)_4(THF)_2]^+$ in toluene and produced two major products, a reduced monoruthenium(II) species (*trans*-$Ru(\eta^2\text{-}O_2CCH_3)_2(PPh_3)_2$) and an oxidized diruthenium(III,III) μ-oxo-bridged complex $(Ru_2(\mu\text{-}O)(\mu_2\text{-}O_2CCH_3)_2(\eta^2\text{-}O_2CCH_3)_2(PPh_3)_2)$, which had been proposed earlier by Mitchell et al.[4] A disproportionation scheme was postulated to explain this product distribution. Chakravarty and co-workers[6−9] looked at similar reactions between $[Ru_2(\mu\text{-}O_2CAr)_4Cl]$ (Ar = aryl) and PPh_3 in CH_3CN and CH_3CN/H_2O mixtures and obtained μ-oxo- and μ-aquo-bridged diruthenium(III,-III) and diruthenium(II,III) complexes (containing no formal Ru−Ru bond) as well as mixed complexes containing a mononuclear Ru(II) cation and an Ru_2(II,-III) or Ru_2(II,II) tetracarboxylate anion, usually with chloride axial ligands. They also found two interesting features in that CH_3CN, a modest π-acid itself, was detected in the equatorial position of many of their products, and in the reactions performed in a CH_3CN/H_2O mix, carboxylates were sometimes bound in an η^1 fashion to an Ru center along with being hydrogen-bonded to a μ-aquo bridge. This latter feature is perhaps a clue to the mechanism of displacement of the carboxylates during the disassembly process.

* Corresponding author. Tel: +902-867-5336. Fax: +902-867-2414. E-mail: maquino@stfx.ca.
[†] St. Francis Xavier University.
[‡] Dalhousie University.

(1) Aquino, M. A. S. *Coord. Chem. Rev.* **1998**, *170*, 141.
(2) Legzdins, P.; Mitchell, P. A.; Rempel, G. L.; Ruddick, J. D.; Wilkinson, G. J. *J. Chem. Soc. A* **1970**, 3322.
(3) Cotton, F. A.; Norman, J. G., Jr. *Inorg. Chim. Acta* **1972**, *6*, 411.
(4) Mitchell, R. W.; Spencer, A.; Wilkinson, G. J. *J. Chem. Soc., Dalton Trans.* **1973**, 846.
(5) Barral, M. C.; Jiménez-Aparicio, R.; Royer, E. C.; Urbanos, F. A.; Monge, A.; Ruiz-Valero, C. *Polyhedron* **1991**, *10*, 113.
(6) Das, B. K.; Chakravarty, A. R. *Inorg. Chem.* **1990**, *29*, 1783.
(7) Das, B. K.; Chakravarty, A. R. *Inorg. Chem.* **1990**, *29*, 2078.
(8) Das, B. K.; Chakravarty, A. R. *Inorg. Chem.* **1991**, *30*, 4978.
(9) Das, B. K.; Chakravarty, A. R. *Inorg. Chem.* **1992**, *31*, 1395.
(10) Boyar, E. B.; Harding, P. A.; Robinson, S. D.; Brock, C. P. *J. Chem. Soc., Dalton Trans.* **1986**, 1771.

10.1021/om049635n CCC: $27.50
Publication on Web 09/23/2004

Only one study to date has looked at the interaction of diphosphines with the $[Ru_2(\mu\text{-}O_2CR)_4]^+$ core. Robinson and co-workers[10] reacted $Ru_2(\mu\text{-}O_2CR)_4Cl$ (R = Me, Et, *t*-Bu, CF_3, and Ph) with bis(diphenylphosphino)methane (dppm), 1,2-bis(diphenylphosphino)ethane (dppe), and 1,3-bis(diphenylphosphino)propane (dppp). Three distinct disassembly products were obtained depending on the solvent used and the temperature of the reaction. In refluxing methanol racemic mixtures of the tris-chelated $[Ru(\eta^2\text{-}O_2CR)(Ph_2P(CH_2)_nPPh_2)_2](BPh_4)$, n = 1−3, product was obtained. In refluxing methanol/benzene (1:1 v/v), *cis*-$Ru(\eta^1\text{-}O_2CR)_2(Ph_2P(CH_2)_nPPh_2)_2$, n = 1−3, was obtained (but only for R = Me and Et), and in the same solvent mixture when the reaction was carried out at room temperature the *trans* product, *trans*-$Ru(\eta^1\text{-}O_2CR)_2(Ph_2P(CH_2)_nPPh_2)_2$, n = 1−3, was produced (but not for R = *t*-Bu). Conversion of the *trans*-$Ru(\eta^1\text{-}O_2CR)_2(Ph_2P(CH_2)_nPPh_2)_2$ complex to the $[Ru(\eta^2\text{-}O_2CR)(Ph_2P(CH_2)_nPPh_2)_2](BPh_4)$ form could be afforded by reacting the latter in methanol/benzene at reflux. However, only one of the complexes, $[Ru(\eta^2\text{-}O_2CCH_3)(Ph_2P(CH_2)PPh_2)_2](BPh_4)$, was structurally characterized. Very recently, Lucas et al.[11] obtained a structure of the acetate-dppe derivative, $[Ru(\eta^2\text{-}O_2CR)(Ph_2P(CH_2)_2PPh_2)_2](PF_6)\cdot 2MeOH$. Their reaction route was quite different from Robinson's in that they began with a mononuclear starting material, *cis*-$RuCl_2(dppe)_2$, which they reacted with sodium acetate and ammonium hexafluorophosphate in refluxing dichloromethane. Subsequent recrystallization was performed from methanol.

Our interest in this research began a few years ago when we were able to isolate an axial phosphine diadduct of the form $[Ru_2(\mu\text{-}O_2CCH_3)_4(PR_3)_2]^+$. This adduct is, presumably, the initial intermediate formed in the disassembly process involving monophosphines. We succeeded in synthesizing and characterizing the diadduct, $[Ru_2(\mu\text{-}O_2CCH_3)_4(PCy_3)_2]^+$ (Cy = cyclohexyl), by using a 2:1 (ligand:metal) reaction ratio, a very short reaction time, and a bulky phosphine.[12] In a parallel line of work we recently synthesized a series of diruthenium(II,III) tetraferrocenecarboxylates in which the equatorially bridging carboxylate R group contained an Fe^{2+} center (R = ferrocenyl, Fc).[13,14] Electrochemical measurements were carried out to investigate any electronic interactions between the essentially *inorganic* Ru_2 core and the *organometallic* ferrocene centers (as well as between the ferrocene centers themselves). The use of ferrocenecarboxylates as ligands is surprisingly sparse,[15] and their coordination to one or more Ru centers is particularly rare. In fact, other than our two papers that structurally characterize three complexes that contain ferrocenecarboxylates μ_2-bound to a dinuclear Ru_2^{5+} center, only one other example of a structurally characterized complex exists. This being the organometallic complex $[Ru(\eta^2\text{-}O_2CFc)(CH{=}CH_2)(CO)(PPh_3)_2]$, in which $FcCOO^-$ is bound in a η^2 fashion to Ru(II), synthesized by Ros and co-workers.[16]

Intended as a follow-up to our previous paper in this journal,[14] the current study builds on these two lines of research and extends and more fully develops Robinson's earlier work on the diphosphine reactions. We report here on the synthesis (using the disassembly process outlined above), structure, and electrochemistry of the heterodinuclear species $[Ru(\eta^2\text{-}O_2CFc)(dpp)_2](PF_6)$, where dpp = dppm, dppe, and dppp. In addition we have resynthesized the three acetate analogues, $[Ru(\eta^2\text{-}O_2CCH_3)(dpp)_2](PF_6)$ (dpp as above), using slightly different starting materials, structurally characterized all three, and thoroughly explored their electrochemistry in order to contrast with the ferrocenyl-containing complexes.

The major goals of this research were (a) to increase the number of structurally characterized ruthenium complexes with ferrocenecarboxylate ligands, (b) to investigate the electrochemistry of, and any interactions between, bimetallic complexes with distinct metal and organometallic redox sites (these types of compounds have recently been referred to as metal-organometallic units (MOMs) by Sweigart and co-workers[17]), and (c) to shed more light on the actual mechanism of disassembly of $[Ru_2(\mu\text{-}O_2CR)_4]^+$-type complexes with π-acids.

Experimental Section

Materials. All reagents were obtained from commercial suppliers and used as received, unless otherwise noted. Dichloromethane and 1,2-dichloroethane were distilled under nitrogen over CaH_2. $[Ru_2(\mu\text{-}O_2CCH_3)_4(H_2O)_2](PF_6)$ was prepared by the method of Drysdale et al.,[18] and $[Ru_2(\mu\text{-}O_2CFc)_4(MeOH)_2](PF_6)$ was prepared according to Cooke et al.[13,14]

Physical Measurements. Infrared spectra were recorded on a Bio-Rad FTS-175 spectrophotometer as KBr disks. ^1H and ^{31}P NMR data were recorded on a Bruker Aspect 300 MHz NMR spectrometer in $CDCl_3$ using tetramethylsilane (TMS) as a reference for ^1H data and phosphoric acid as the reference for the ^{31}P spectra. Cyclic voltammetry (CV) and Osteryoung square wave voltammetry (OSWV) were performed in 1,2-dichloroethane or dichloromethane using a BAS CV-50 voltammetric analyzer. The cell system consisted of a platinum button working electrode, a platinum wire auxiliary electrode, and an Ag/AgCl reference electrode. The ferrocenium/ferrocene couple was used as an internal reference and found to have an $E_{1/2}$ = 440 mV vs Ag/AgCl (ΔE = 65 mV, scan rate = 100 mV s^{-1}). Measurements were normally performed on a 2 mM solution of the complex with 0.100 M tetrabutylammonium hexafluorophosphate, $[CH_3(CH_2)_3]_4NPF_6$ (TBAH), as the supporting electrolyte. All solutions were purged with argon for 15 min prior to each scan. Elemental analyses were performed by Canadian Microanalytical Service Ltd., Delta, B.C., Canada. X-ray data were collected at the DalX X-ray facility, Dalhousie University, Halifax, N.S., Canada.

$[Ru(\eta^2\text{-}O_2CCH_3)(dppm)_2](PF_6)\cdot MeOH$ (1). $[Ru_2(\mu\text{-}O_2CCH_3)_4(H_2O)_2](PF_6)$ (0.100 g, 0.148 mmol) and a 4-fold excess of bis(diphenylphosphino)methane (dppm) (0.228 g, 0.593 mmol) were dissolved in 120 mL of methanol and refluxed under argon for 8 h. As the reaction progressed, the solution gradually changed in color from brown to red to yellow. When the reflux was complete, ammonium hexafluorophosphate (0.024 g, 0.148 mmol) was added and the volume reduced under vacuum to 20 mL. The solution was allowed to cool at

(11) Lucas, N. T.; Powell, C. E.; Humphrey, M. G. *Acta Crystallogr., Sect. C* **2000**, *C56*, e392.
(12) Briand, G. G.; Cooke, M. W.; Cameron, T. S.; Farrell, H. M.; Burchell, T. J.; Aquino, M. A. S. *Inorg. Chem.* **2001**, *40*, 3267.
(13) Cooke, M. W.; Murphy, C. A.; Cameron, T. S.; Swarts, J. C.; Aquino, M. A. S. *Inorg. Chem. Commun.* **2000**, *3*, 721.
(14) Cooke, M. W.; Cameron, T. S.; Robertson, K. N.; Swarts, J. C.; Aquino, M. A. S. *Organometallics* **2002**, *21*, 5962.
(15) Aquino, M. A. S.; Wyman, I. W. *Trends Inorg. Chem.* **2004**, *8*, 1.
(16) Matas, L.; Moldes, I.; Soler, J.; Ros, J.; Larena, A.; Piniella, J. F. *Organometallics* **1998**, *17*, 4551.
(17) Oh, M.; Carpenter, G. B.; Sweigart, D. A. *J. Chem. Soc., Chem. Commun.* **2002**, 2168.
(18) Drysdale, K. D.; Beck, E. J.; Cameron, T. S.; Robertson, K. N.; Aquino, M. A. S. *Inorg. Chim. Acta* **1997**, *256*, 243.

−10 °C overnight, producing a crystalline yellow precipitate, which was filtered, washed with a small amount of ice cold methanol, and dried in vacuo. Yield = 0.237 g (72%). Anal. Calcd (%) for $RuC_{52}H_{47}O_2P_5F_6 \cdot CH_3OH$: C, 57.56; H, 4.65; P, 14.00. Found: C, 57.85; H, 4.39; P, 13.75. IR (cm^{-1}): 3442 (w), 3061 (w), 2928 (w), 1463 (s), 1436 (s), 1188 (w), 1162 (w), 1102 (s), 1000 (w), 839 (s), 784 (w), 732 (m), 615 (m), 510 (m), 461 (m). NMR in $CDCl_3$, ^1H (δ/ppm): 7.8−6.9, 6.17 (multiplet, 40 phenyl protons); 4.63, 4.04 (multiplet, 4 methylene protons); 1.77 (singlet, 3 methyl protons). ^{31}P (δ/ppm): −5.69 (triplet, 2P); −13.77 (triplet, 2P); −146.38 (septet, 1P).

[Ru(η^2-O_2CCH_3)(dppe)$_2$](PF$_6$) (2). 2 was prepared in a fashion similar to **1** except that 1,2-bis(diphenylphosphino)-ethane (dppe) (0.237 g, 0.595 mmol) was used (instead of dppm). Yield = 0.268 g (82%). Anal. Calcd (%) for $RuC_{54}H_{51}O_2P_5F_6$: C, 58.86; H, 4.67; P, 14.05. Found: C, 58.75; H, 4.76; P, 14.26. IR (cm^{-1}): 3442 (w), 3061 (w), 2928 (w), 1467 (s), 1436 (s), 1098 (s), 839 (s), 746 (m), 694 (s), 557 (m), 527 (m), 454 (m). NMR in $CDCl_3$, ^1H (δ/ppm): 7.8−6.9, 5.84 (multiplet, 40 phenyl protons); 3.0, 2.3, 2.0, 1.56 (multiplet, 8 ethylene protons); 0.52 (singlet, 3 methyl protons). ^{31}P (δ/ppm): 57.02 (triplet, 2P); 55.32 (triplet, 2P); −146.49 (septet, 1P).

[Ru(η^2-O_2CCH_3)(dppp)$_2$](PF$_6$) (3). 3 was prepared in a fashion similar to **1** except that 1,3-bis(diphenylphosphino)-propane (dppp) (0.245 g, 0.594 mmol) was used. Yield = 0.254 g (76%). Anal. Calcd (%) for $RuC_{56}H_{55}O_2P_5F_6$: C, 59.53; H, 4.91; P, 13.71. Found: C, 59.16; H, 5.04; P, 14.05. IR (cm^{-1}): 3432 (w), 3063 (w), 2922 (w), 2871 (w), 1471 (s), 1436 (s), 1165 (m), 1092 (s), 1029 (m), 974 (m), 838 (s), 747 (m), 698 (s), 650 (m), 557 (m), 508 (s), 460 (m). NMR in $CDCl_3$, ^1H (δ/ppm): 7.7−6.7 (multiplet, 40 phenyl protons); 2.6, 1.8, 1.56, 1.2 (multiplet, 12 propylene protons); 1.40 (singlet, 3 methyl protons). ^{31}P (δ/ppm): 31.13 (triplet, 2P), 2.56 (triplet, 2P), −143.21 (septet, 1P).

[Ru(η^2-O_2CFc)(dppm)$_2$](PF$_6$) (4). [Ru$_2$(μ-$O_2CFc)_4$(MeOH)$_2$]-(PF$_6$) (0.100 g, 0.074 mmol) and a 4-fold excess of dppm (0.114 g, 0.297 mmol) were dissolved in 120 mL of methanol and refluxed under argon for 8 h. The solution color changed from a rust-red to a golden orange-yellow as the reflux proceeded. At the end of the reflux 0.012 g (0.074 mmol) of NH_4PF_6 was added and the solution reduced in volume under vacuum to between 20 and 30 mL. After cooling at −10 °C overnight the microcrystalline orange solid was filtered, washed with a small amount of ice-cold methanol, and dried in vacuo. Yield = 0.129 g (70%). Anal. Calcd (%) for $RuFeC_{61}H_{53}O_2P_5F_6$: C, 58.90; H, 4.29; P, 12.45; Fe, 4.49. Found: C, 58.62; H, 4.51; P, 12.80; Fe, 4.27. IR (cm^{-1}): 3442 (w), 3058 (w), 2923 (w), 1510 (s), 1481 (s), 1436 (s), 1362 (m), 1190 (m), 1098 (s), 1026 (m), 1001 (m), 837 (s), 784 (m), 735 (s), 697 (s), 557 (m), 509 (s), 484 (m). NMR in $CDCl_3$, ^1H (δ/ppm): 7.9−6.9, 6.10 (multiplet, 40 phenyl protons); 4.5, 3.9 (multiplet, 4 methylene protons); 4.7−4.3 (multiplet, 4 bound Cp ring protons); 3.8 (singlet, 5 unbound Cp ring protons). ^{31}P (δ/ppm): 3.69 (triplet, 2P), −17.96 (triplet, 2P), −148.59 (septet, 1P).

[Ru(η^2-O_2CFc)(dppe)$_2$](PF$_6$) (5). 5 was prepared in a manner similar to **4** except that dppe (0.118 g, 0.298 mmol) was used. Yield = 0.137 g (73%). Anal. Calcd (%) for $RuFeC_{63}H_{57}O_2P_5F_6$: C, 59.49; H, 4.52; P, 12.18; Fe, 4.39. Found: C, 59.08; H, 4.40; P, 12.49; Fe, 4.26. IR (cm^{-1}): 3436 (w), 3061 (w), 2931 (w), 1508 (s), 1482 (s), 1436 (s), 1403 (s), 1364 (m), 1193 (w), 1099 (m), 1027 (m), 1001 (m), 840 (s), 746 (m), 699 (s), 557 (m), 527 (s), 482 (m). NMR in $CDCl_3$, ^1H (δ/ppm): 7.9−7.1, 6.18 (multiplet, 40 phenyl protons); 3.4, 2.3, 2.1, 1.6 (multiplet, 8 ethylene protons); 4.4−4.0 (multiplet, 4 bound Cp ring protons); 3.7 (singlet, 5 unbound Cp ring protons). ^{31}P (δ/ppm): 57.66 (triplet, 2P), 51.35 (triplet, 2P), −143.76 (septet, 1P).

[Ru(η^2-O_2CFc)(dppp)$_2$](PF$_6$) (6). 6 was prepared in a fashion similar to **4** except that dppp (0.125 g, 0.303 mmol) was used. Yield = 0.154 g (79%). Anal. Calcd (%) for $RuFeC_{65}H_{61}O_2P_5F_6$: C, 60.06; H, 4.73; P, 11.91; Fe, 4.30. Found: C, 59.71; H, 4.62; P, 12.25; Fe, 4.39. IR (cm^{-1}): 3449 (w), 3058 (w), 2933 (w), 2871 (w), 1508 (s), 1483 (m), 1435 (s), 1404 (m), 1364 (w), 1194 (w), 1160 (w), 1091 (m), 1002 (w), 974 (w), 839 (s), 746 (m), 697 (s), 558 (m), 512 (s), 483 (w). NMR in $CDCl_3$, ^1H (δ/ppm): 7.7−6.7 (multiplet, 40 phenyl protons); 2.6, 2.0, 1.6, 1.2 (multiplet, 12 propylene protons); 4.6−4.2 (multiplet, 4 bound Cp ring protons); 3.59 (singlet, 5 unbound Cp ring protons). ^{31}P (δ/ppm): 22.42 (triplet, 2P), 4.01 (triplet, 2P), −143.72 (septet, 1P).

X-ray Crystallography. Crystals for all complexes, **1**−**6**, were obtained in one of two ways, either by slow evaporation from a methanol solution or by diethyl ether diffusion into a 1,2-dichloroethane solution of the complex. X-ray diffraction was performed using a Rigaku AFC5R diffractometer equipped with a rotating anode generator. Cu Kα radiation was used for complexes **1** and **2** and Mo Kα radiation for complexes **3**−**6**. No decay corrections were applied. An empirical absorption correction based on azimuthal scans of several reflections was applied. The structures were solved by direct methods, using SIR 92[19] for **3** and SHELX97[20] for the rest, and expanded using Fourier techniques.[21] The final cycle of full-matrix least-squares refinement was based on the observed reflections ($I > 3.00\sigma(I)$) and the variable parameters and converged with unweighted (R) and weighted agreement factors (R_w). Neutral atom scattering factors were from Cromer and Waber.[22] Anomalous dispersion effects were included in F_{calc},[23] and the values of $\Delta f'$ and $\Delta f''$ were from Creagh and McAuley.[24] The values of the mass attenuation coefficients are from Creagh and Hubbell.[25] The data were corrected for Lorentz and polarization effects. All calculations were performed using the teXsan software package from Molecular Structure Corporation.[26] For structures **1**, **2**, **5**, and **6** the non-hydrogen atoms were refined anisotropically. For structures **3** and **4** some non-hydrogen atoms, particularly Ru, P, F, and O, were refined anisotropically, while the rest (particularly C) were refined isotropically. Hydrogen atoms were included but not refined. In structures **4** and **5** the anion (PF_6^-) was disordered, and all six of the fluoride atoms were allowed to occupy two positions (each with occupancies of 0.5 and equal atomic displacement parameters for each A/B pair). The P−F bond lengths were restrained to 1.58(2) Å, and the *trans* F···F bond lengths were restrained to 3.16(2) Å. A rigid bond restraint was also applied to the P−F bonds of the anion.

Results and Discussion

Synthesis. The syntheses of all the [Ru(η^2-O_2CR)-(dpp)$_2$](PF$_6$) type complexes (**1**−**6**) in this report were carried out in a fashion similar to the method of Robinson[10] in refluxing methanol with two notable differences. The starting tetracarboxylate used was of the diadduct form, [Ru$_2$(μ-$O_2CR)_4$(L)$_2$](PF$_6$) (where R = CH_3, L = H_2O; R = Fc, L = MeOH), instead of the

(19) SIR92. Altomare, A.; Cascarano, M.; Giacovazzo, C.; Guagliardi, A. *J. Appl. Crystallogr.* **1994**, *26*, 343.
(20) Sheldrick, G. M. *SHELX97*, 1997.
(21) Beurskens, P. T.; Admiraal, G.; Beurskens, G.; Bosman, W. P.; de Gelder, R.; Israel, R.; Smits, J. M. M. *DIRDIF94*, The DIRDIF-94 program system, Technical Report of the Crystallography Laboratory; University of Nijmegen: The Netherlands, 1994.
(22) Cromer, D. T.; Waber, J. T. *International Tables for X-Ray Crystallography*; The Kynoch Press: Birmingham, England, 1974; Vol. IV, Table 2.2A.
(23) Ibers, J. A.; Hamilton, W. C. *Acta Crystallogr.* **1964**, *17*, 781.
(24) Creagh, D. C.; McAuley, W. J. In *International Tables for Crystallography*; Wilson, A. J. C., Ed.; Kluwer Academic Publishers: Boston, 1992; Vol. C, Table 4.2.6.8, pp 219−222.
(25) Creagh, D. C.; Hubbell, J. H. In *International Tables for Crystallography*; Wilson, A. J. C., Ed.; Kluwer Academic Publishers: Boston, 1992; Vol. C, Table 4.2.4.3, pp 200−206.
(26) *teXsan for Windows version 1.06*, Crystal Structure Analysis Package; Molecular Structure Corporation, 1997−1999.

Table 1. ^{31}P NMR Data

complex	δ(P, diphosphine)/ppm[a]	J(PP′)/Hz	δ(P, PF_6^-)/ppm[a]	J(PF)/Hz	spin system
1	−5.69 (t), −13.77 (t)	39.10	−146.38 (sept)	712	A_2X_2[b]
4	3.69 (t), −17.96 (t)	39.28	−148.59 (sept)	712	A_2X_2[b]
2	57.02 (t), 55.32 (t)	18.12	−146.49 (sept)	713	A_2B_2
5	57.66 (t), 51.35 (t)	19.08	−143.76 (sept)	713	A_2X_2[b]
3	31.13 (t), 2.56 (t)	31.65	−143.21 (sept)	711	A_2X_2[b]
6	22.42 (t), 4.01 (t)	32.42	−143.72 (sept)	712	A_2X_2[b]

[a] t = triplet, sept = septet. [b] Possibly AA′XX′ (see text).

chloro-bridged polymer, and refluxing was carried out for a period of 8 h instead of 1 h. The former change afforded a more soluble starting reagent, and both changes presumably led to somewhat higher yields. During the course of the reaction the color changed from red-brown to yellow for the acetate derivatives and to an orange color for the ferrocenecarboxylate complexes. The addition of 1 or more molar equiv of NH_4PF_6 to the final reaction solution was important, as it provided the additional PF_6^- counterion for the 2 molar equiv of the mononuclear ruthenium(II) product that was produced. The overall reaction is given in eq I; however, a more detailed assessment of the mechanism is left until later (vide infra). It should be noted here that CO_2 was detected as an additional product of the reaction.

$$[Ru_2(\mu\text{-}O_2CR)_4(L)_2](PF_6) + 4\ dpp \xrightarrow{PF_6^-} 2\ [Ru(\eta^2\text{-}O_2CR)(dpp)_2](PF_6)\ (\mathbf{1}-\mathbf{6}) + CO_2 + 2\ L + \text{other uncharacterized products (H, C, O)} \quad (1)$$

Yields ranged from 70 to 82%, and all six complexes gave satisfactory elemental analyses.

IR and NMR Spectroscopy. The infrared spectra of all the complexes displayed the typical symmetric (ν_{sym}) and asymmetric (ν_{asym}) carboxylate stretching frequencies in the range 1435−1485 cm^{-1} with $\Delta\nu$ ranging from 30 to 50 cm^{-1}, indicative of a η^2 binding mode.[27] The separations in the ferrocenecarboxylate-containing complexes **4**−**6** tended to be slightly larger than in the acetate derivatives, **1**−**3**. The characteristic P−F stretch of the PF_6^- counterion was seen at ∼840 cm^{-1} for all the complexes.[27] In addition, alkane C−H stretching modes are seen at 2922−2938 cm^{-1} for the acetate complexes and weak phenyl-ring C−H stretches in the range 3061−3108 cm^{-1} for all complexes. Finally a metal to Cp-ring stretch band is seen in all of the ferrocenyl derivatives at 482−484 cm^{-1}.

Both ^{31}P and ^{1}H NMR spectra were run in $CDCl_3$ for all the complexes. The ^{31}P spectra of complexes **1**−**3** showed features for the bound diphenylphosphine ligands similar to those seen by Robinson.[10] A pair of triplets is seen for the two pairs of equivalent phosphorus centers. The spectra of complexes **4**−**6** are similar and can be assigned in an analogous fashion to the acetate complexes with the equivalent diphenylphosphine groups. Chemical shifts (δ), coupling constants, and splitting patterns are reported in Table 1. (The complexes are grouped in pairs with the same diphosphine ligands.) The splitting patterns for complexes **1** and **3** are consistent with an A_2X_2 assignment; however complex **2**, which contains the dppe ligand, is closer to an A_2B_2 pattern, as also seen by Robinson ($\Delta\nu/J$ = 9.5). In contrast, all of the ferrocenecarboxylate complexes, **4**−**6**, are consistent with an A_2X_2 pattern, even the dppe-containing **5**, which has $\Delta\nu/J$ = 33.5.

Table 2. ^{1}H NMR Data

complex	δ(CH_3 or Fc protons)/ppm[a]	δ(CH_2 protons)/ppm[a]	δ(phenyl protons)/ppm
1	1.77 (s)	4.04, 4.63	6.17, 6.9−7.8
4	3.8 (s), 3.9, 4.3, 4.7	3.9, 4.5	6.10, 6.9−7.95
2	0.52 (s)	1.56, 2.0 (t), 2.3, 3.0	5.84, 6.9−7.9
5	3.7 (s), 4.0, 4.1, 4.3, 4.4	1.6, 2.1, 2.3, 3.4	6.18, 7.1−8.0
3	1.40 (s)	1.2, 1.56, 1.8, 2.6	6.7−7.7
6	3.59 (s), 4.18, 4.31, 4.58	1.2, 1.6, 2.0, 2.6	6.7−7.7

[a] s = singlet, t = triplet.

It should be noted here that there may be some ambiguity in the assignment of the splitting pattern. In Table 2 of Robinson's paper (ref 10) the dppe−acetate complex is assigned to an A_2B_2 pattern and the dppm and dppp derivatives show triplets with the implication of an A_2X_2 pattern. However, in the text of their paper they imply the pattern to be AA′XX′ for all three compounds. Our crystal structure of **2** (see Supporting Information) shows that both Ru−P(*trans* to O) bonds are equal by symmetry, as are both Ru−P(*trans* to P) bonds, forcing an A_2B_2 pattern. This is not the case for complexes **1** and **3**, where there is some inequity in these respective bond lengths, and an AA′XX′ may be a more rigorous assignment. Despite this, only two triplets are seen (as in Robinson's case), which implies the slight inequity in the bond lengths averages out in solution. For complexes **4**−**6** this bond inequity is only slightly more pronounced in the crystal structures and the ferrocenyl group is free to rotate about the Cp−carboxyl carbon bond, and again a pair of triplets is seen. So, while we do not rule out an AA′XX′ pattern, in these instances the spectra very closely resemble an A_2X_2 splitting.

As our counterion, PF_6^-, differed from that of Robinson (who used BPh_4^-), we also see a characteristic septet due to the phosphorus−fluorine coupling, J(PF). The chemical shifts for these are in the range −143.2 to −148.6 ppm with J(PF) ≈ 712 Hz.

The ^{1}H NMR data are reported in Table 2. The spectra for the acetate derivatives, **1**−**3**, show chemical shift values similar to those seen by Robinson, with phenyl protons falling in the range 5.8−7.8 ppm and methylene protons in the range 1.2−4.6 ppm. The methyl protons are generally the furthest upfield and display singlets at 1.77, 0.52, and 1.40 for **1**, **2**, and **3**, respectively. The ferrocenyl analogues show phenyl ring protons in a range similar to their acetate cousins at 6.1−8.0 ppm as well as methylene protons in the range 1.2−4.5 ppm. Ferrocenyl protons are normally at lower chemical shifts (further downfield) than typical phenyl aromatic systems due to the shielding effect of the metal

(27) Nakamoto, K. *Infrared and Raman Spectra of Inorganic and Coordination Compounds, Part B*, 5th ed.; John Wiley and Sons: New York, NY, 1997.

Table 3. Crystal Data for Complexes 1−6

	1·MeOH	**2**·2H_2O	**3**·MeOH	**4**	**5**·2MeOH	**6**
empirical formula	$C_{52}H_{47}F_6O_2P_5Ru$	$C_{27}H_{27.50}O_2P_{2.50}Ru_{0.50}F_3$	$C_{57}H_{59}O_3P_5RuF_6$	$RuC_{61}H_{53}O_2FeP_5F_6$	$C_{65}H_{65}O_4F_6Fe_1P_5Ru_1$	$C_{65}H_{61}F_6Fe_1O_2P_5Ru_1$
formula mass (g/mol)	1073.87	568.98	1162.02	1243.86	1335.94	1299.97
temperature (°C)	23	23	-90	23	-130	23
cryst dimens (mm)	0.19 × 0.17 × 0.10	0.04 × 0.15 × 0.40	0.12 × 0.13 × 0.27	1.20 × 0.70 × 0.40	0.52 × 0.39 × 0.31	1.00 × 0.80 × 0.40
cryst syst	monoclinic	monoclinic	monoclinic	orthorhombic	triclinic	monoclinic
lattice type	primitive	C-centered	primitive	primitive	primitive	primitive
space group	*P*2/*c*	*C*2/*c*	$P2_1$	$Pna2_1$	$P\bar{1}$	$P2_1/c$
a (Å)	13.069(2)	13.632(2)	11.609(4)	20.355 (4)	15.011(7)	14.166(2)
b (Å)	11.007(2)	19.576(1)	14.963(2)	13.803 (2)	17.103(5)	20.123(2)
c (Å)	34.101(6)	20.295(4)	15.202(1)	20.100 (6)	13.088(8)	20.6052(9)
α (deg)					104.47(4)	
β (deg)	90.43(1)	98.22(1)	99.29(1)	90.0(5)	103.76(4)	96.453(7)
γ (deg)					67.98(3)	
Z (molecules/cell)	4	8	2	4	2	4
volume (Å^3)	4905(1)	5360(1)	2606.0(8)	5647 (2)	2977(3)	5836(1)
D_{calc} (g/cm^3)	1.45	1.410	1.481	1.463	1.49	1.48
radiation (*λ*, Å)	1.5418(Cu Kα)	1.54178(Cu Kα)	0.71069(Mo Kα)	0.7107(Mo Kα)	0.71069(Mo Kα)	0.71069(Mo Kα)
$2\theta_{max.}$ (deg)	127.5	127.2	60.1	60.1	60.2	60.1
no. of reflns measd	8846	10085	8369	5842	18 084	18 204
no. of unique reflns	7974	4482	7912	5842	17 470	17 563
no. of obsd reflns	7964	1928	4347	5441	17 470	17 102
no. of params	597	320	359	281	741	739
refln/param ratio	13.34	6.03	12.11	19.36	23.58	950.11
R_f ($I > 3\sigma(I)$)[a]	0.0831	0.038	0.045	0.0588	0.0464	0.0499
R_w[b]	0.2069	0.040	0.054	0.1531	0.1374	0.1144
goodness of fit[c]	1.301	1.54	1.05	0.927	1.026	0.926

[a] $R_f = \sum||F_o| - |F_c||/\sum|F_o|$. [b] $R_w = [\sum w(|F_o| - |F_c|)^2/\sum wF_o^2]^{1/2}$. [c] Goodness of fit = $[\sum w(|F_o| - |F_c|)^2/$(no. of observed reflections − no. of parameters)$]^{1/2}$.

electrons and are normally seen around 4 ppm. The unbound Cp ring protons appear as a singlet, whereas the bound Cp ring (containing the carboxyl group) protons appear as multiplets in the same area.

X-ray Structures. X-ray structures were obtained for all complexes, **1**−**6**, normally by slow evaporation from methanol or by diffusion of diethyl ether into a 1,2-dichloroethane solution of the complex. All of the complexes assume a certain degree of distorted octahedral geometry with two *cis*-chelating diphosphine ligands and a bidentate (η^2) carboxylate. To some extent, certainly for the acetate derivatives, the carboxylate lies in a "cavity" of the phenyl rings on adjacent phosphines. It should also be noted that all of the complexes exist as racemic mixtures of Δ and Λ stereoisomers. The crystal data for complexes **1**−**6** are given in Table 3.

[Ru(η^2-O_2CCH_3)(dppm)$_2$](PF_6) (1). As mentioned in the Introduction, Robinson[10] has reported the structure of the BPh_4^- salt of complex **1**, and we report our structure here only for confirmation and comparison purposes, as our structure is poorer than Robinson's. While our space group was *P*2/*c* and his was $P\bar{1}$, the key bond lengths and angles are all reasonably similar. For example, a comparison of our bond lengths and angles with Robinson's (in parentheses) are as follows: Ru−O = 2.21 Å (2.187 and 2.197 Å), Ru−P (*trans* to P) = 2.357 and 2.389 Å (2.342 and 2.347 Å), Ru−P (*trans* to O) = 2.256 and 2.278 Å (2.277 and 2.292 Å), O−Ru−O = 59.6° (59.4°), and P−Ru−P = 70.2° and 70.5° (71.80° and 72.26°). The small deviations that do exist could be due to the different counterion. A structural diagram of **1** and a full listing of bond lengths and angles are given in the Supporting Information.

[Ru(η^2-O_2CCH_3)(dppe)$_2$](PF_6)·2H_2O (2·2H_2O). As already noted, the dimethanol solvate of this complex was prepared by Lucas[11] from the *cis*-Ru(dppe)$_2Cl_2$ starting material and structurally characterized. The quality of both structures is comparable (our *R*-value was 0.038 and Lucas' was 0.035), and the space groups were the same (*C*2/*c*). As with **1**, the inclusion of this structure is instructive for confirmation and comparison purposes. Some key bond lengths and angles (with Lucas' values in parentheses) are as follows: Ru−O = 2.198 Å (not reported by Lucas), Ru−P (*trans* to P) = 2.385 Å (2.3785 Å), Ru−P *(trans* to O) = 2.310 Å (2.3074 Å), O−Ru−O = 58.7° (59.43°), and P−Ru−P = 82.43° (not reported). In this case it is possible that small deviations are due to the different molecules of solvation. A drawing of **2** and a full listing of bond lengths and angles are given in the Supporting Information.

[Ru(η^2-O_2CCH_3)(dppp)$_2$](PF_6)·MeOH (3·MeOH). Complex **3**·MeOH crystallizes in the monoclinic space group $P2_1$ and has a methanol of solvation present. The dppp ligands form a six-membered ring with the metal center, and the bite angle is now around 90°. As in **1** and **2**, the acetate bite angle remains close to 60° and the acetate group sits in a distinct cavity formed by the phenyl rings of the diphosphine ligands (Figure 1). Selected bond lengths and angles for **3** are reported in Table 4.

[Ru(η^2-O_2CFc)(dppm)$_2$](PF_6) (4). The first of the ferreocenecarboxylate-containing complexes, **4** crystal-

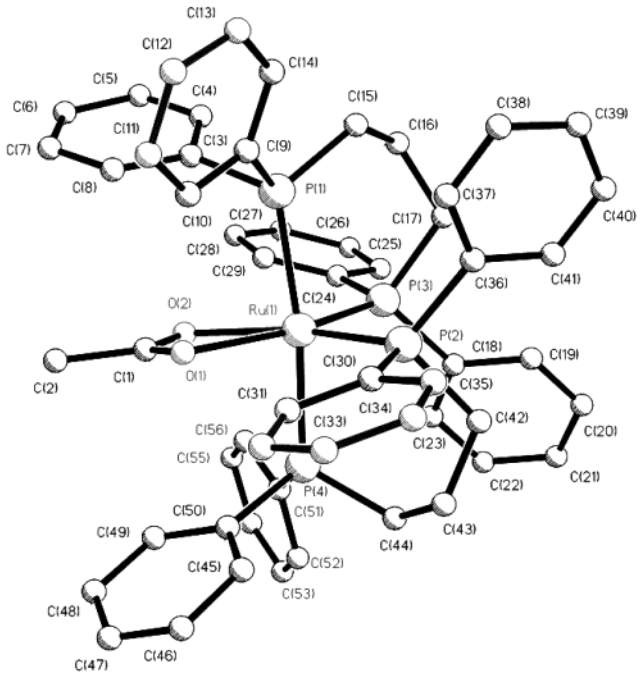

Figure 1. Molecular structure of $[Ru(\eta^2\text{-}O_2CCH_3)(dppp)_2]^+$, $\mathbf{3}^+$. The methanol of solvation and the PF_6^- counterion were omitted for clarity.

Table 4. Selected Bond Lengths (Å) and Angles (deg) for $[Ru(\eta^2\text{-}O_2CCH_3)(dppp)_2](PF_6)\cdot MeOH$, 3·MeOH

Ru(1)−O(1)	2.232(6)	P(3)−C(18)	1.848(9)
Ru(1)−O(2)	2.221(6)	P(3)−C(24)	1.857(9)
Ru(1)−P(2)	2.316(2)	P(4)−C(44)	1.827(9)
Ru(1)−P(3)	2.318(2)	P(4)−C(50)	1.838(8)
Ru(1)−P(1)	2.430(2)	P(4)−C(51)	1.847(9)
Ru(1)−P(4)	2.416(2)	C(15)−C(16)	1.54(1)
P(1)−C(3)	1.836(9)	C(16)−C(17)	1.53(1)
P(1)−C(9)	1.850(8)	C(42)−C(43)	1.51(1)
P(1)−C(15)	1.828(9)	C(43)−C(44)	1.53(1)
P(2)−C(30)	1.837(8)	O(1)−C(1)	1.25(1)
P(2)−C(36)	1.834(9)	O(2)−C(1)	1.28(1)
P(2)−C(42)	1.833(9)	C(1)−C(2)	1.49(1)
P(3)−C(17)	1.838(9)		
O(1)−Ru(1)−O(2)	58.4(2)	P(2)−Ru(1)−O(2)	162.5(2)
P(1)−Ru(1)−P(3)	90.12(8)	P(3)−Ru(1)−O(1)	161.5(2)
P(2)−Ru(1)−P(4)	90.60(8)	P(2)−Ru(1)−P(3)	93.73(7)
Ru(1)−O(1)−C(1)	91.7(5)	P(3)−Ru(1)−P(4)	94.37(8)
Ru(1)−O(2)−C(1)	91.4(5)	P(1)−Ru(1)−O(1)	86.9(2)
O(1)−C(1)−C(2)	120.7(8)	P(2)−Ru(1)−O(1)	104.7(2)
O(2)−C(1)−C(2)	120.8(8)	P(4)−Ru(1)−O(1)	87.0(2)
O(1)−C(1)−O(2)	118.5(8)	P(1)−Ru(1)−O(2)	88.6(2)
P(1)−Ru(1)−P(2)	95.04(8)	P(3)−Ru(1)−O(2)	103.4(2)
P(1)−Ru(1)−P(4)	172.56(9)	P(4)−Ru(1)−O(2)	84.6(2)

lizes in the orthorhombic space group $Pna2_1$. While the carboxyl group still sits in a slight cavity formed by the phenyl rings, the ferrocenyl group protrudes well enough out of it (see Figure 2). As with all of the acetate derivatives, the carboxylate bite angle is close to 60° and the diphosphine (dppm) bite angle is 70.1−70.7°, which is essentially identical to that seen in **1**. A selection of bond lengths and angles are reported in Table 5.

$[Ru(\eta^2\text{-}O_2CFc)(dppe)_2](PF_6)\cdot 2MeOH$ (5·2MeOH). Complex **5**·MeOH crystallizes in the triclinic space group $P\bar{1}$ and contains two molecules of solvated methanol. This complex has features similar to those of **2** and **4** with a carboxylate bite angle around 60° and the larger five-membered ring formed by the dppe ligand leading to a larger bite angle of 82−83° (versus 70° for the dppm derivative), as seen in **2**. The structure of **5** is

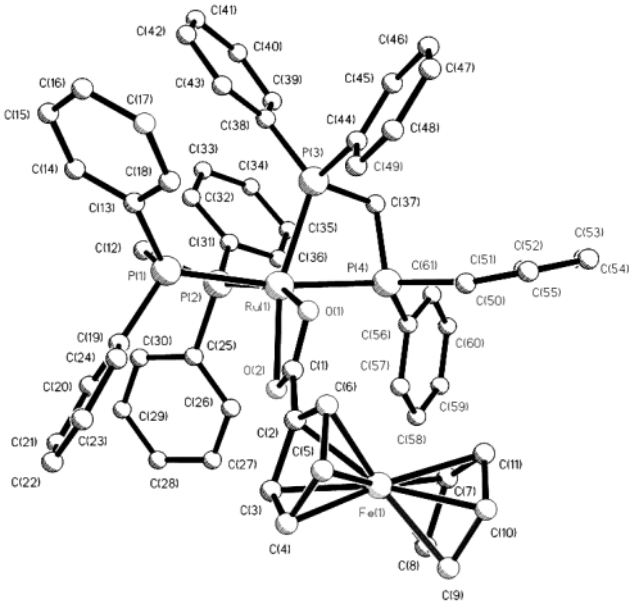

Figure 2. Molecular structure of $[Ru(\eta^2\text{-}O_2CFc)(dppm)_2]^+$, $\mathbf{4}^+$. The PF_6^- counterion was omitted for clarity.

Table 5. Selected Bond Lengths (Å) and Angles (deg) for $[Ru(\eta^2\text{-}O_2CFc)(dppm)_2](PF_6)$, 4

Ru(1)−O(1)	2.17(1)	P(2)−C(12)	P(2)−C(12)
Ru(1)−O(2)	2.21(3)	P(2)−C(25)	P(2)−C(25)
Ru(1)−P(2)	2.30(2)	P(2)−C(31)	P(2)−C(31)
Ru(1)−P(3)	2.31(2)	P(3)−C(37)	P(3)−C(37)
Ru(1)−P(1)	2.339(8)	P(3)−C(38)	P(3)−C(38)
Ru(1)−P(4)	2.398(6)	P(3)−C(44)	P(3)−C(44)
Fe(1)−C(2)	2.02(3)	P(4)−C(37)	P(4)−C(37)
Fe(1)−C(3)	2.03(2)	P(4)−C(50)	P(4)−C(50)
Fe(1)−C(4)	2.02(2)	P(4)−C(56)	P(4)−C(56)
Fe(1)−C(7)	2.06(2)	O(1)−C(1)	O(1)−C(1)
P(1)−C(12)	1.83(2)	O(2)−C(1)	O(2)−C(1)
P(1)−C(13)	1.80(2)	C(1)−C(2)	C(1)−C(2)
P(1)−C(19)	1.81(2)		
O(1)−Ru(1)−O(2)	61(1)	O(2)−Ru(1)−P(3)	160.7(5)
P(2)−Ru(1)−P(1)[a]	70.7(3)	P(2)−Ru(1)−P(3)	94(2)
P(3)−Ru(1)−P(4)[a]	70.1(7)	P(2)−Ru(1)−P(4)	101.4(3)
Ru(1)−O(1)−C(1)	90(2)	P(3)−Ru(1)−P(1)	100.8(8)
Ru(1)−O(2)−C(1)	87(2)	O(1)−Ru(1)−P(1)	91.8(4)
P(1)−Ru(1)−C(1)	89.9(8)	O(1)−Ru(1)−P(3)	104(2)
P(4)−Ru(1)−C(1)	102.0(7)	O(1)−Ru(1)−P(4)	98.0(4)
P(2)−Ru(1)−C(1)	132.5(8)	O(2)−Ru(1)−P(1)	91.4(9)
P(3)−Ru(1)−C(1)	132.9(13)	O(2)−Ru(1)−P(2)	104(1)
C(1)−C(2)−Fe(1)	125(2)	O(2)−Ru(1)−P(4)	99.5(8)
O(1)−C(1)−C(2)	116(3)	O(1)−C(1)−C(2)	116(3)
O(2)−C(1)−C(2)	122(2)	O(2)−C(1)−C(2)	122(2)
P(1)−Ru(1)−P(4)	168.0(3)	C(3)−C(2)−C(1)	128(2)
O(1)−Ru(1)−P(2)	157.3(5)	C(6)−C(2)−C(1)	124(2)

shown in Figure 3. Selected bond lengths and angles are given in Table 6.

$[Ru(\eta^2\text{-}O_2CFc)(dppp)_2](PF_6)$ (6). Finally, **6** crystallizes in the monoclinic space group $P2_1/c$ and displays features similar to **3** with a carboxylate bite angle of 60° and a diphosphine bite angle of 88.6−89.4° (due to the larger six-membered ring). A drawing of **6** is shown in Figure 4**,** and selected bond lengths and angles are listed in Table 7.

Structural Trends. It would seem useful at this point to summarize some of the structural trends seen in complexes **1**−**6** rather than discussing each parameter for each individual case. It is clear from what we have said above that the carboxylate bite angle, whether for acetate or ferrocenecarboxylate, is invariant at around 60°. The diphosphine bite angle is invariant of the carboxylate group present and increases only as the

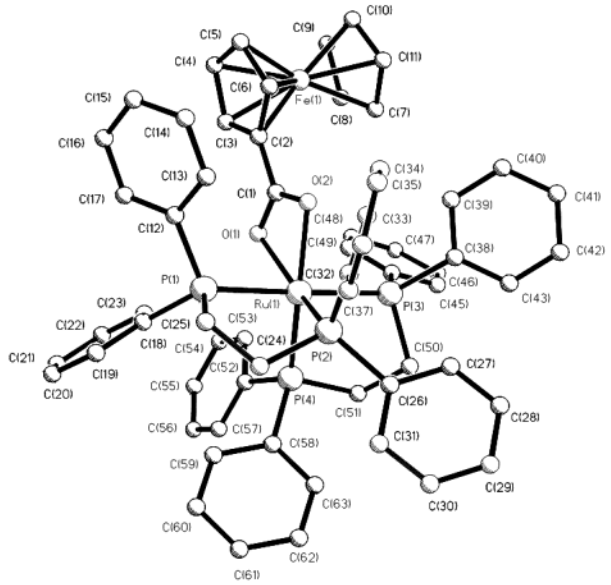

Figure 3. Molecular structure of $[Ru(\eta^2\text{-}O_2CFc)(dppe)_2]^+$, $\mathbf{5}^+$. The methanols of solvation and the PF_6^- counterion were omitted for clarity.

Table 6. Selected Bond Lengths (Å) and Angles (deg) for $[Ru(\eta^2\text{-}O_2CFc)(dppe)_2](PF_6)\cdot 2MeOH$, 5·2MeOH

Ru(1)−O(1)	2.211(2)	P(2)−C(26)	1.826(3)
Ru(1)−O(2)	2.161(2)	P(2)−C(32)	1.845(3)
Ru(1)−P(2)	2.299(2)	C(24)−C(25)	1.527(4)
Ru(1)−P(4)	2.309(1)	P(3)−C(38)	1.820(3)
Ru(1)−P(1)	2.370(1)	P(3)−C(44)	1.849(3)
Ru(1)−P(3)	2.389(1)	P(3)−C(50)	1.839(3)
Fe(1)−C(2)	2.039(3)	P(4)−C(51)	1.862(3)
Fe(1)−C(3)	2.047(3)	P(4)−C(52)	1.843(3)
Fe(1)−C(4)	2.063(4)	P(4)−C(58)	1.828(3)
Fe(1)−C(7)	2.056(4)	C(50)−C(51)	1.520(4)
P(1)−C(12)	1.835(3)	O(1)−C(1)	1.281(3)
P(1)−C(18)	1.825(3)	O(2)−C(1)	1.268(3)
P(1)−C(25)	1.841(3)	C(1)−C(2)	1.455(4)
P(2)−C(24)	1.844(3)		

O(2)−Ru(1)−O(1)	59.89(8)	O(2)−Ru(1)−P(4)	163.47(6)
P(2)−Ru(1)−P(1)	82.67(5)	P(2)−Ru(1)−P(3)	98.25(5)
P(4)−Ru(1)−P(3)	82.86(5)	P(2)−Ru(1)−P(4)	93.89(5)
Ru(1)−O(1)−C(1)	89.7(2)	P(4)−Ru(1)−P(1)	98.28(5)
Ru(1)−O(2)−C(1)	92.4(2)	O(1)−Ru(1)−P(1)	82.45(7)
P(1)−Ru(1)−C(1)	83.87(8)	O(1)−Ru(1)−P(3)	96.32(7)
P(3)−Ru(1)−C(1)	94.64(8)	O(1)−Ru(1)−P(4)	106.10(6)
P(2)−Ru(1)−C(1)	129.77(7)	O(2)−Ru(1)−P(1)	88.88(7)
P(4)−Ru(1)−C(1)	135.94(7)	O(2)−Ru(1)−P(2)	101.82(7)
C(1)−C(2)−Fe(1)	130.1(2)	O(2)−Ru(1)−P(3)	89.77(7)
O(1)−C(1)−C(2)	121.5(2)	O(1)−C(1)−C(2)	121.5(2)
O(2)−C(1)−C(2)	120.7(2)	O(2)−C(1)−C(2)	120.7(2)
P(1)−Ru(1)−P(3)	178.50(2)	C(3)−C(2)−C(1)	126.0(3)
O(1)−Ru(1)−P(2)	156.55(6)	C(6)−C(2)−C(1)	125.4(3)

ring size increases from four-membered (70.1−70.7°) to five-membered (82.4−82.9°) to six-membered (88.6−90.6°).

The Ru−O bond lengths show no discernible trends for complexes **1**−**3**, remaining fairly constant at 2.20−2.23 Å with symmetrical binding of the OCO group in **1** and **2** and essentially symmetrical binding (within error) in **3** (Ru(1)−O(1) = 2.232(6) Å, Ru(1)−O(2) = 2.221(6) Å). The ferreocenecarboxylate complexes **4**−**6** display a slightly larger range in Ru−O bond lengths (2.16−2.21 Å), and hence there is a slightly greater degree of asymmetry in the binding. The values of the

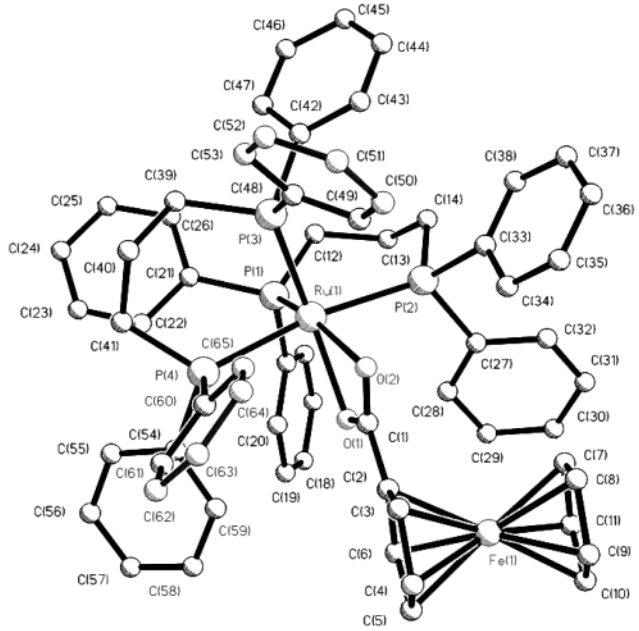

Figure 4. Molecular structure of $[Ru(\eta^2\text{-}O_2CFc)(dppp)_2]^+$, $\mathbf{6}^+$. The PF_6^- counterion was omitted for clarity.

Table 7. Selected Bond Lengths (Å) and Angles (deg) for $[Ru(\eta^2\text{-}O_2CFc)(dppp)_2](PF_6)$, 6

Ru(1)−O(1)	2.173(4)	P(2)−C(33)	1.855(7)
Ru(1)−O(2)	2.200(4)	C(12)−C(13)	1.523(9)
Ru(1)−P(1)	2.326(2)	C(13)−C(14)	1.534(9)
Ru(1)−P(3)	2.311(2)	P(3)−C(39)	1.838(6)
Ru(1)−P(2)	2.418(2)	P(3)−C(42)	1.849(7)
Ru(1)−P(4)	2.481(2)	P(3)−C(48)	1.846(7)
Fe(1)−C(2)	2.047(6)	P(4)−C(41)	1.830(6)
Fe(1)−C(3)	2.027(7)	P(4)−C(54)	1.836(6)
Fe(1)−C(4)	2.040(7)	P(4)−C(60)	1.843(7)
Fe(1)−C(7)	2.041(7)	C(39)−C(40)	1.519(8)
P(1)−C(12)	1.819(6)	C(40)−C(41)	1.536(9)
P(1)−C(15)	1.841(6)	O(1)−C(1)	1.275(7)
P(1)−C(21)	1.843(7)	O(2)−C(1)	1.277(7)
P(2)−C(14)	1.839(6)	C(1)−C(2)	1.437(8)
P(2)−C(27)	1.837(7)		

O(1)−Ru(1)−O(2)	60.0(2)	O(1)−Ru(1)−P(3)	163.0(1)
P(1)−Ru(1)−P(2)	89.35(6)	O(2)−Ru(1)−P(1)	161.0(1)
P(3)−Ru(1)−P(4)	88.56(6)	P(3)−Ru(1)−P(1)	94.30(6)
Ru(1)−O(1)−C(1)	91.4(4)	P(3)−Ru(1)−P(2)	97.46(6)
Ru(1)−O(2)−C(1)	90.1(4)	O(1)−Ru(1)−P(1)	101.8(1)
P(2)−Ru(1)−C(1)	88.5(2)	O(1)−Ru(1)−P(2)	88.4(1)
P(4)−Ru(1)−C(1)	80.71(14)	O(1)−Ru(1)−P(4)	83.4(1)
P(1)−Ru(1)−C(1)	131.8(2)	O(2)−Ru(1)−P(2)	85.1(1)
P(3)−Ru(1)−C(1)	133.7(2)	O(2)−Ru(1)−P(3)	104.4(1)
C(1)−C(2)−Fe(1)	130.9(4)	O(2)−Ru(1)−P(4)	84.5(1)
O(1)−C(1)−C(2)	120.3(6)	O(1)−C(1)−C(2)	120.3(6)
O(2)−C(1)−C(2)	121.7(6)	O(2)−C(1)−C(2)	121.7(6)
P(1)−Ru(1)−P(4)	99.39(6)	C(3)−C(2)−C(1)	126.9(6)
P(2)−Ru(1)−P(4)	169.02(6)	C(1)−C(2)−C(6)	126.3(6)

respective Ru−O bonds are within error of each other for **4** (just) but are slightly different in **5** (Ru(1)−O(1) = 2.211(2) Å, Ru(1)−O(2) = 2.161(2) Å) and **6** (Ru(1)−O(1) = 2.173(4) Å, Ru(1)−O(2) = 2.200(4) Å). The reason for these slight asymmetries is unclear but may be due to weak interactions of the ferrocenyl group with adjacent phenyl rings. In the only previous structure of an Ru(II) complex with η^2-coordinated ferrocencarboxylate, Ros' $[Ru(\eta^2\text{-}O_2CFc)(CH{=}CH_2)(CO)(PPh_3)_2]$ complex, the Ru−O bond lengths are somewhat more asymmetric, at 2.269(3) and 2.192(3) Å, than in any of our systems. (The carboxylate bite angle was 58.7(1)° and comparable to ours.)

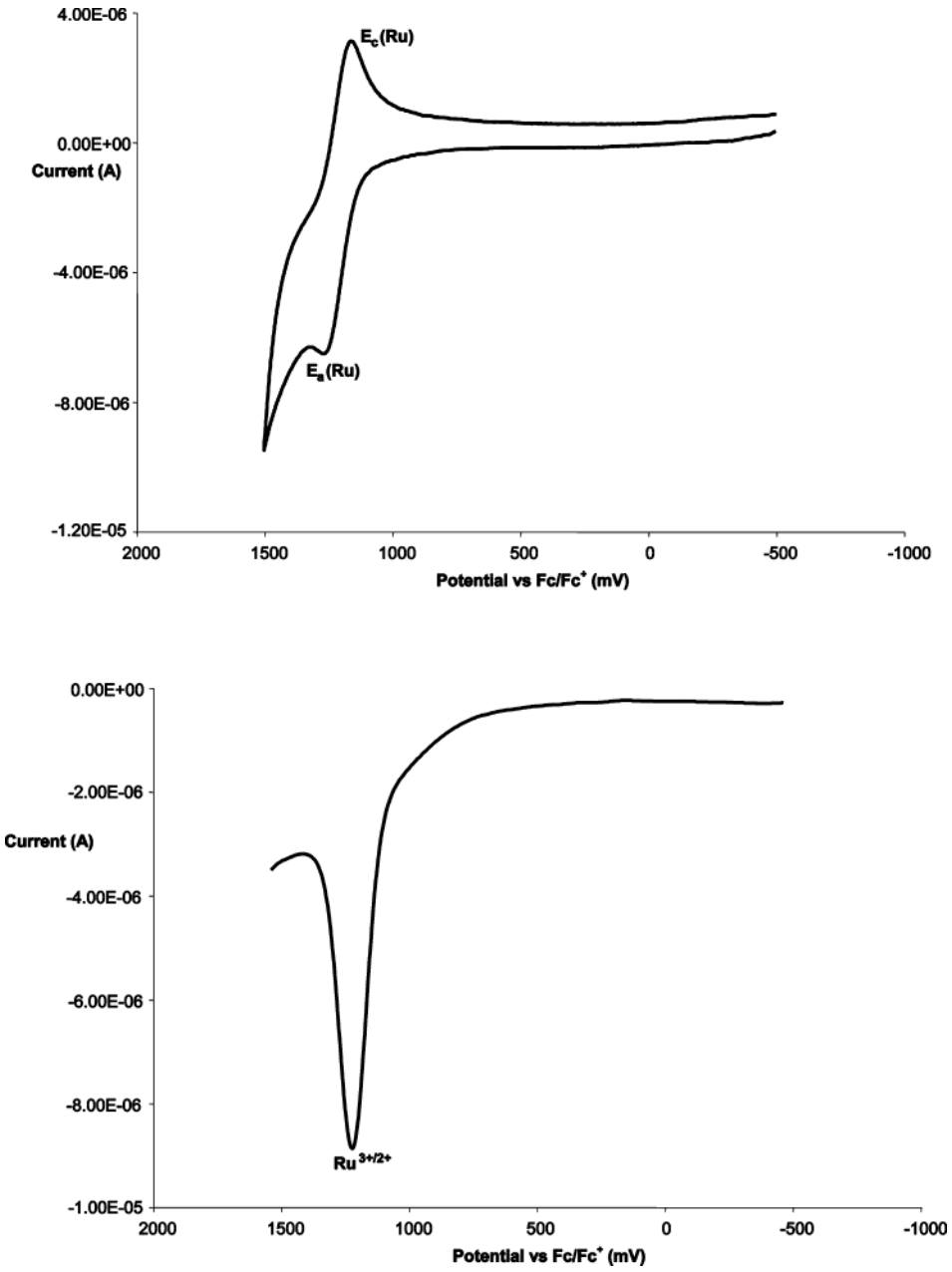

Figure 5. Cyclic voltammogram (top) and Osteryoung square wave voltammogram of [Ru(η^2-O_2CCH_3)(dppe)$_2$](PF_6), **2**.

There are two types of Ru−P bonds: those *trans* to another phosphorus and those that are *trans* to a carboxyl oxygen, with the former being longer in all cases due to the *trans*-influence. The Ru−P (*trans* to P) bond lengths range from 2.339(8) to 2.481(2) Å and those *trans* to O from 2.256 to 2.326(2) Å. No major trends are discernible except that the Ru−P bonds (*trans* to P) are longest in the two dppp complexes **3** and **6** (>2.41 Å).

The carboxyl carbon to Cp carbon bond length in complexes **4**−**6** ranges from 1.437(8) to 1.50(3) Å and is slightly less than that for a pure single bond, indicating that there may be a small degree of conjugation between the ferrocene and the carboxyl group. (Ros' complex had a C−C bond length of 1.463(7) Å.)

Finally, the Cp rings on the ferrocenes of complexes **4**−**6** do not deviate significantly from the eclipsed conformations. The angles are 8(2)° for **4**, 2.6(3)° for **5**, and 0(1)° for **6**. The deviations are most likely less than that seen in the [Ru_2(μ-O_2CFc)$_4$($MeOH$)$_2$](PF_6) starting material as the twist angles for an analogous complex, [Ru_2(μ-O_2CFc)$_4$(n-$PrOH$)$_2$](PF_6), vary from 8° to 16° over the four ferrocenyl groups.[13,14] and are significantly less than the staggered conformation (angle = 19.0°) adopted by Ros' complex.

Electrochemistry. Both cyclic voltammetry (CV) and Osteryoung square-wave voltammetry (OSWV) measurements were performed on all six complexes. These measurements were carried out in dichloromethane or 1,2-dichloroethane (the complexes were more soluble in the latter solvent), and the ferrocenium/ferrocene couple, used as an internal standard, was found to lie at 440 mV vs Ag/AgCl in 1,2-dichloroethane. Figure 5 shows a representative CV and OSWV scan of one of the three acetate derivatives, **2**. The CV shows a one-electron oxidation process (confirmed by coulometry) with $E_{1/2}$ = 1.21 V vs $Fc^{+/0}$, corresponding to the

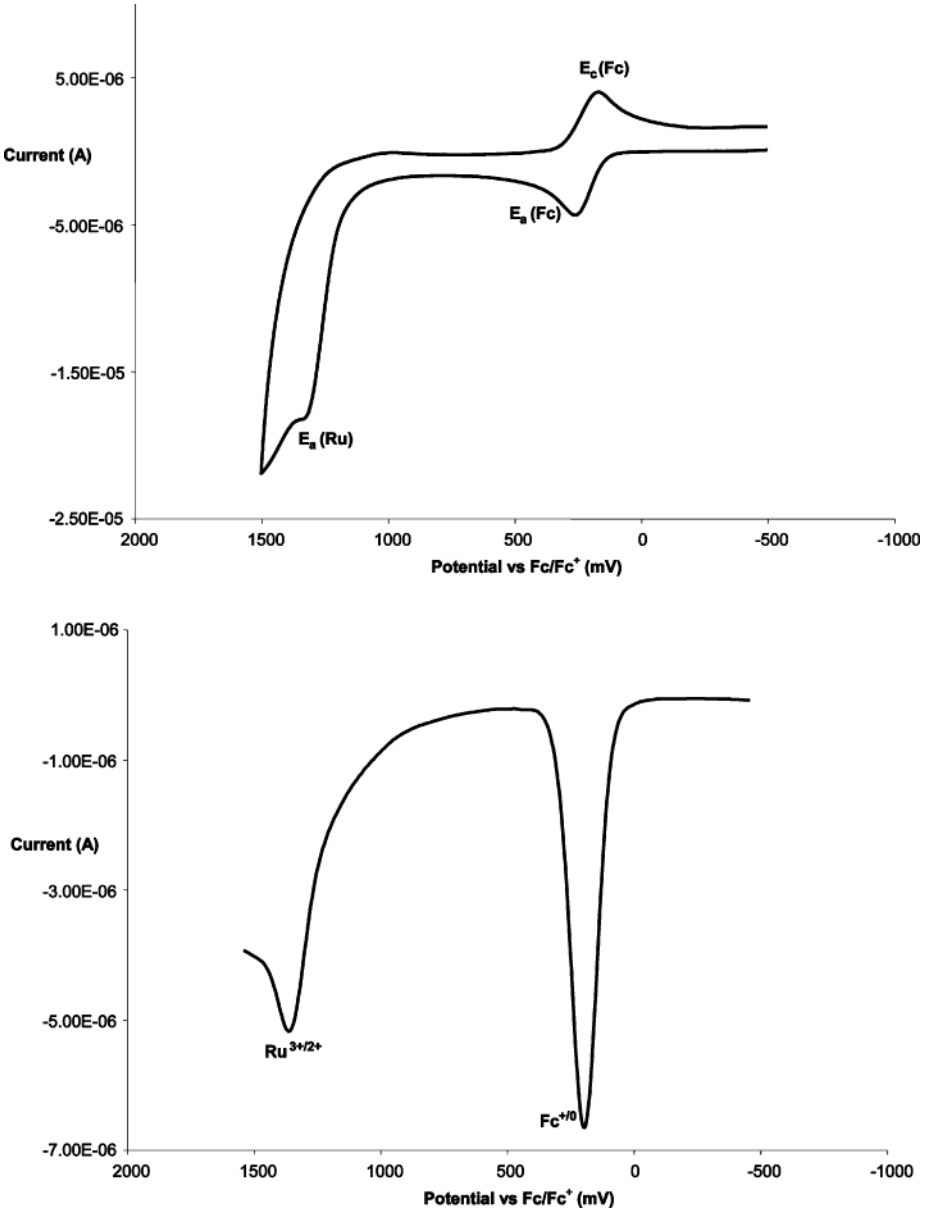

Figure 6. Cyclic voltammogram (top) and Osteryoung square wave voltammogram of [Ru(η^2-O_2CFc)(dppm)$_2$](PF_6), **4**.

oxidation of the ruthenium center, i.e., Ru^{2+} to Ru^{3+}. The OSWV (bottom of Figure 5) confirms this, showing an oxidation wave centered at 1.22 V. The corresponding anodic to cathodic current ratio from the CV for **2** is 1.1, indicating chemical reversibility; however the anodic to cathodic peak separation is 98 mV at 100 mV/s scan rate, and this separation increases as the scan rate increases, implying an electrochemically quasi-reversible process. As one goes to the six-membered diphosphine ring system of [Ru(η^2-O_2CCH_3)(dppp)$_2$](PF_6), **3**, some chemical reversibility is lost as $i_a/i_c = 1.6$ (presumably due to the less stable six- versus five-membered ring), and chemical reversibility is essentially lost ($i_a/i_c = 63$) in complex **1**, which contains the less favored four-membered chelate ring. Five-membered ring chelates involving dppe have been documented to be morefavored than four-, six-, or higher-membered rings,[28] which should lead them to being less likely to undergo significant bond rearrangements during the redox process, hence preserving chemical reversibility.

Figure 6 shows the CV and OSWV of the representative ferrocenecarboxylate-containing complex, [Ru(η^2-O_2CFc)(dppm)$_2$](PF_6), **4**. The CV and OSWV data for complexes **1**−**6** are listed in Table 8. Complexes **4**−**6** display two distinct differences in their electrochemical behavior over those of their acetate analogues.

First, the most distinct difference is the appearance of a one-electron oxidation process corresponding to the $Fe^{3+/2+}$ couple of the ferrocenecarboxylate moiety. This process was found to be chemically reversible (electrochemically quasi-reversible) for all three complexes, **4**−**6**, and to lie in the range of $E_{1/2} = 0.192-0.245$ V, with good agreement between values obtained from CV and those determined from OSWV measurements. The CV and OSWV values obtained for complex **6** are similar to those of the free ferrocenecarboxylic acid, which was reported to be 0.234 V,[14] but the $E_{1/2}$ values for complexes **4** and **5** are slightly less.

(28) Puddephatt, R. J. *Chem. Soc. Rev.* **1983**, 99, and references therein.

Table 8. CV and OSWV Data for Complexes 1−6[a]

	cyclic voltammetry ($Ru^{3+/2+}$)				cyclic voltammetry ($Fe^{3+/2+}$)				OSWV ($Ru^{3+/2+}$)	OSWV ($Fe^{3+/2+}$)
complex	E_a [E_c][b]	ΔE[c]	$E_{1/2}$	(i_a/i_c)[d]	E_a [E_c]	ΔE	$E_{1/2}$	(i_a/i_c)	$E_{1/2}$	$E_{1/2}$
1	1.24	0.283	n/o	62.7					1.16	
2	1.26	0.098	1.21	1.16					1.22	
3	1.32	0.103	1.27	1.67					1.26	
4	1.33 [n/o]	n/o	n/o	n/o	0.262 [0.173]	0.089	0.218	1.16	1.28	0.212
5	1.45 [n/o]	n/o	n/o	n/o	0.235 [0.149]	0.086	0.192	1.02	1.35	0.193
6	1.43 [n/o]	n/o	n/o	n/o	0.298 [0.210]	0.088	0.245	1.02	1.32	0.240

[a] All measurements carried out in 1,2-dichloroethane at 25 °C with 0.100 TBAH at a scan rate of 100 mV s^{-1}. All entries are given in V vs the $Fc^{+/0}$. [b] Anodic [E_a] and cathodic [E_c] potentials where observed. n/o = not observed. [c] $E_a - E_c$ where observed. [d] Anodic to cathodic peak current ratios where observed.

Second, any chemical reversibility in the core $Ru^{3+/2+}$ couple is completely lost in the CVs of all three complexes, and only an anodic (E_a) wave is seen corresponding to the oxidation of the core from Ru^{2+} to Ru^{3+}, with no visible cathodic peak (E_c). This could possibly be due to a re-reduction of the Ru^{3+} that is generated by any other unoxidized ferrocenecarboxylate moieties attached as ligands in other complexes.[29] This was partly verified by adding free ferrocene to a solution of complex **2**, which, as discussed above, displayed a reversible $Ru^{3+/2+}$ couple. The addition of the ferrocene caused an immediate loss of the cathodic current. Similar behavior was seen for **3**. (The process in **1** was already irreversible.) We were able to determine $E_{1/2}$ values for this couple from the OSWV, and in all cases the value was somewhat higher than the value for the corresponding complexes **1**−**3** with the same diphosphine ligand. This increase in the difficulty to oxidize the ruthenium core is mostly due to the charge effect (proximity of Fe(III) to the Ru(II) center); however, it is also possible that there is a small degree of metal−metal interaction in the Ru(II)Fe(III) mixed-valent state of complexes **4**−**6**, which could lead to a shift in $E_{1/2}$.

Looking at the values in a bit more detail, of the three heterobimetallic complexes, **5** displays the largest separation between the metal redox potentials in the OSWV with $E_{1/2}(Ru^{3+/2+}) - E_{1/2}(Fe^{3+/2+}) = 1.16$ V (versus 1.07 V for **4** and 1.08 V for **6**). This "mixed-valent" stability is primarily due to the inherent dissymmetry (different metal environments) than to any metal−metal interactions; however, the difference between the $E_{1/2}(Ru^{3+/2+})$ value for **2** and the free ferrocenecarboxylic acid (fca) value of 0.234 V is about 0.99 V (the difference is about 0.93 V for **1** and free fca and 1.03 V for **3** and free fca). This leads to an additional increase in electrochemical stabilization of the "mixed-valent" heterobimetallic species, over the various mononuclear ruthenium(II) acetate fragments and the free ferrocenecarboxylic acid fragment, of approximately 170 mV for **5**, 140 mV for **4**, and 50 mV for **6**. To be able to truly determine if some of this modest stabilization is due to metal−metal interactions or all due to a charge effect, we are attempting to isolate the mixed-valent Ru(II)Fe(III) species and perform detailed UV−visible spectroscopic and electrospectroscopic studies on them.

Proposed Mechanism of Disassembly. We would like to propose a reasonable mechanism for the disassembly of the mixed-valent diruthenium tetracarboxylate core by the bidentate phosphine ligands used here as well as in Robinson's earlier study. The mechanism here is not based on the disproportionation reaction proposed previously by Jiménez-Aparicio[5] since in all cases our yields of mononuclear ruthenium(II) product were well over 50%. Scheme 1 outlines the proposed mechanism.

In addition to being good π-acids, phosphines are also good σ-bases, and the initial step involves the *axial* substitution of the labile solvent (methanol) with one arm of the phosphine. This initial step has been proposed by others; however, more direct evidence came from recent work in our lab in which we isolated and structurally characterized the *axial* phosphine diadduct $[Ru_2(\mu\text{-}O_2CCH_3)_4(PCy_3)_2]^+$ (as mentioned in the Introduction). The second step would involve the displacement of one arm of each of two carboxylates (in *equatorial* positions) by the loose arm of the *axially* bound diphosphines. The next step is the most complicated and least defined and essentially involves three processes, the order of which we are currently not entirely clear on. There appears to be reductive decarboxylation of one of the monodentately bound carboxylates (and a simple loss of the other) as well as an *equatorial* migration of the originally *axially* bound end of the phosphine and *axial* binding of the second set of diphosphine ligands. It is possible that the binding of the additional phosphine drives the other two processes to occur, but this requires more study. There is certainly evidence from theoretical studies[30] that π-acids (phosphines in particular) prefer the *equatorial* sites over the *axial* sites, as there appears to be a larger distribution of π electron density from the dimetal centers in this direction. Experimentally, particularly in Jiménez-Aparicio and Chakravarty's studies mentioned earlier, the π-acids end up in the *equatorial* positions. There is evidence for the reductive decarboxylation from liquid crystal and thermal analysis studies carried out by Cukiernik and co-workers[31−33] in which loss of carboxylate, oxidation to CO_2, and slow decomposition of the resulting diruthenium(II,II) species resulted at moderate temperatures. We have detected CO_2 being produced during all of our reactions; however, for this to occur, the radicals $RCO_2^\bullet$ and subsequently $R^\bullet$ should be

(29) A referee has suggested that the peak may be a catalytic peak resulting from the reaction of Ru(III)/Fe(III) with Ru(II)/Fe(III), giving two Ru(III)/Fe(II), which would be oxidized at the potential of $E_{a(Ru)}$ (more positive than $E_{a(Fe)}$) and so on. This would be a multielectron process which disagrees with our coulometry and, due to the closeness of the process to the solvent cutoff, would be difficult to verify.

(30) Norman, J. G.; Renzoni, G. E.; Case, D. A. *J. Am. Chem. Soc.* **1979**, *101*, 5256.
(31) Cukiernik, F. D.; Ibn-Elhaj, M.; Chaia, Z. D.; Marchon, J. C.; Giroud-Godquin, A. M.; Guillon, D.; Skoulios, A.; Maldivi, P. *Chem. Mater.* **1998**, *10*, 83.
(32) Rusjan, M. C.; Sileo, E. E.; Cukiernik, F. D. *Solid State Ionics* **1999**, *124*, 143.
(33) Rusjan, M. C.; Sileo, E. E.; Cukiernik, F. D. *Solid State Ionics* **2003**, *159*, 389.

Scheme 1. Proposed Mechanism of Disassembly of the $[Ru_2(\mu\text{-}O_2CR)_4(MeOH)_2]^+$ Dimer by Diphosphines

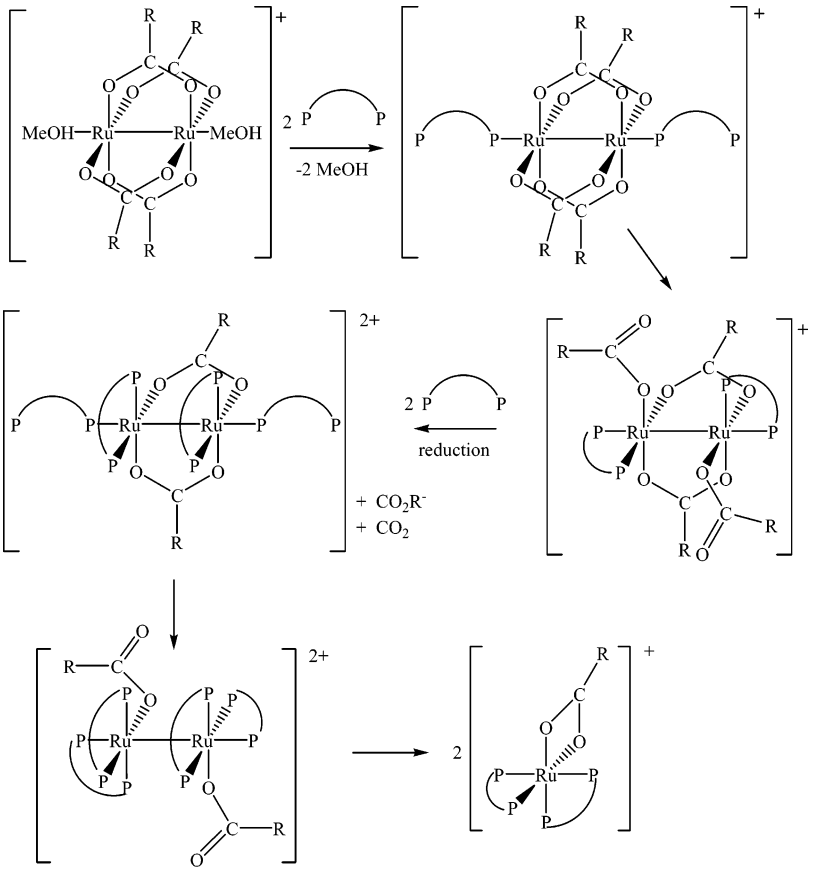

generated, which we do not detect (they may be too transient). The second possibility is reduction by a diphosphine. This would seem unlikely, as all the reactions are stoichiometric (4:1 ligand:metal), and for the ligand to act as reductant at least 25% of the diphosphines should be oxidized to the diposphine oxide. As the yields of three of the six compounds are greater than 75% and we detect no phosphine oxide in the product, this pathway for reduction seems unlikely. More work is needed to fully elucidate the mechanism of reduction. In the penultimate step the free phosphine end of the second set of diphosphines displaces one arm of each of the remaining carboxylates. The Ru−Ru bond is so weakened by the loss of bridging ligands and, possibly, the loss of bonding π-electron density to the phosphines and the addition of antibonding electron density from the same phosphines that it breaks and the vacant coordination site is occupied by the remaining carboxylate on each Ru. We thus end up with 2 mol of the racemic $\Delta\Lambda$-$[Ru(\eta^2\text{-}O_2CR)(dpp)_2]^+$ species. Some additional support for our mechanism, at least for the substitutional processes the diphosphines undergo, has recently been demonstrated by Sasaki[34] in the partial displacement of carboxylates by pyridylamino ligands on the $Rh_2(\mu\text{-}O_2CCH_3)_4(MeOH)_2$ species. Equatorial substitution on diruthenium cores (versus dirhodium) is usually more facile and there is no ultimate cleavage of the dirhodium bond in Sasaki's case.

(34) Yoshimura, T.; Umakoshi, K.; Sasaki, Y. *Inorg. Chem.* **2003**, *42*, 71106.

Conclusion

We have fully characterized three η^2-bound ferrocenecarboxylatoruthenium(II) complexes (where only one had existed to date) via a useful disassembly reaction of the $[Ru_2(\mu\text{-}O_2CFc)_4]^+$ core with diphosphine ligands. These complexes are unique from the previous example in that they provide both a metal and an organometallic site (MOM). Their electrochemical properties have been studied and compared to the corresponding acetatoruthenium(II) analogues. The heterobimetallic species display not only a very stable mixed-valent state ($\Delta E_{1/2}$ > 1.0 V) but also an increased stability versus the isolated mononuclear fragments, particularly for the most stable five-membered dppe-ring system. Further spectroscopic studies have been initiated to detect any metal−metal interactions that may be present. Isolation and characterization of the mixed-valent species are currently underway.

A preliminary mechanism of the disassembly process has also been outlined. This should provide a good starting point to build on; however, more fundamentally, the entire disassembly process may provide a unique reaction pathway to otherwise difficult to synthesize monoruthenium(II) complexes. While the acetate derivatives can be synthesized from $Ru(dpp)_2Cl_2$ starting materials, as Lucas has done,[11] early indications from our lab show that the ferrocenecarboxylate derivatives can be produced only in low yields (<20%) and require longer reaction times (>16 h) when prepared by this route. The assessment of the uniqueness of this methodology is also underway.

CCDC deposition numbers 237969−237974.

Acknowledgment. M.A.S.A. thanks NSERC (Canada) for financial support.

Supporting Information Available: Structural diagrams for complexes **1** and **2**, X-ray data tables for **1**−**6**, and X-ray crystallographic files (CIF) for complexes **1**−**6**. This material is available free of charge via the Internet at http://pubs.acs.org.

OM049635N